Role of Central Nervous System Glucagon-Like Peptide-1 Receptors in Enteric Glucose Sensing

Claude Knauf,[1] Patrice D. Cani,[1,2] Dong-Hoon Kim,[3] Miguel A. Iglesias,[1] Chantal Chabo,[1] Aurélie Waget,[1] André Colom,[1] Sophie Rastrelli,[1] Nathalie M. Delzenne,[2] Daniel J. Drucker,[4] Randy J. Seeley,[3] and Remy Burcelin[1]

OBJECTIVE—Ingested glucose is detected by specialized sensors in the enteric/hepatoportal vein, which send neural signals to the brain, which in turn regulates key peripheral tissues. Hence, impairment in the control of enteric-neural glucose sensing could contribute to disordered glucose homeostasis. The aim of this study was to determine the cells in the brain targeted by the activation of the enteric glucose-sensing system.

RESEARCH DESIGN AND METHODS—We selectively activated the axis in mice using a low-rate intragastric glucose infusion in wild-type and glucagon-like peptide-1 (GLP-1) receptor knockout mice, neuropeptide Y– and proopiomelanocortin–green fluorescent protein–expressing mice, and high-fat diet diabetic mice. We quantified the whole-body glucose utilization rate and the pattern of c-Fos positive in the brain.

RESULTS—Enteric glucose increased muscle glycogen synthesis by 30% and regulates c-Fos expression in the brainstem and the hypothalamus. Moreover, the synthesis of muscle glycogen was diminished after central infusion of the GLP-1 receptor (GLP-1Rc) antagonist Exendin 9-39 and abolished in GLP-1Rc knockout mice. Gut-glucose–sensitive c-Fos–positive cells of the arcuate nucleus colocalized with neuropeptide Y–positive neurons but not with proopiomelanocortin-positive neurons. Furthermore, high-fat feeding prevented the enteric activation of c-Fos expression.

CONCLUSIONS—We conclude that the gut-glucose sensor modulates peripheral glucose metabolism through a nutrient-sensitive mechanism, which requires brain GLP-1Rc signaling and is impaired during diabetes. *Diabetes* 57:2603–2612, 2008

Blood glucose levels are regulated by a dynamic interaction between a number of key organ systems. The gut is the first organ involved in glucose homeostasis because it is the conduit by which carbohydrate enters the body. Digested carbohydrate is transported from the intestinal lumen to the mesenteric vein, then distributed via the hepatoportal vein to the liver, and then distributed to the rest of the body. In the enteric area, which includes intestinal luminal cells and the mesenteric and hepatoportal veins, glucose is detected by specialized cells, i.e., enteric glucose sensors. These sensors transmit signals of endocrine and neuronal origin to peripheral tissues (1–5). Many of the neuronal signals are communicated via the vagus nerve to the brain stem (6,7), which relays the glucose signal to hypothalamic nuclei and then on to pertinent target cells. As an example, Mithieux et al. (8) reported a novel mechanism connecting the portal-sensing macronutrient composition of diet to food intake. This mechanism implies that some of the energy absorbed by the intestine is transformed into glucose by gluconeogenesis. Then, specialized cells of the hepatoportal vein that communicate with the vagus nerve are able to detect glucose and send a signal toward the brain for the control of food intake. Nevertheless, the molecular signals required for the function of the gut-brain axis are incompletely understood.

The incretin glucagon-like peptide-1 (GLP-1) is a candidate regulator of neuronal networks controlling glucose homeostasis. GLP-1 is secreted by enteroendocrine L cells and enhances glucose-stimulated insulin secretion (9). Of direct clinical relevance, both GLP-1 receptor (GLP-1Rc) agonists (9) and dipeptidyl peptidase IV (DPP-IV) inhibitors are now used to treat type 2 diabetes via potentiation of GLP-1 action.

Endogenously secreted GLP-1 acts in the hepatic portal vein to increase the firing rate of the vagus nerve (10,11) and regulate glucose metabolism (12–14). GLP-1 is also secreted by neuronal cells from the caudal region of the brain stem, the nucleus of the tractus solitarius (NTS) (15,16), and released in various hypothalamic, hippocampal, and cortical nuclei, areas that contain functional GLP-1Rcs (15,17–22). Hence, GLP-1 is also considered a neuropeptide, but the control of neural GLP-1 signals in the regulation of glucose homeostasis is poorly understood. To more precisely understand the signals conveyed by enteric glucose sensors, we infused glucose into the mouse stomach at a low rate that resulted in no increase in circulating glucose levels and therefore allowed for the activation of enteric, but not systemic or brain, glucose sensors. We show that under these conditions, whole-body glucose utilization and muscle glycogen synthesis were increased, accompanied by increased c-Fos expression in the brain stem and reduced c-Fos expression in key hypothalamic nuclei. Furthermore, these actions were significantly diminished in GLP-1Rc knockout mice or after brain infusion of a GLP-1Rc antagonist. Immunohistochemical studies revealed that the neuronal population targeted by the enteric glucose signal in the arcuate nucleus (ARC) of the hypothalamus appears to be composed of neuropeptide Y (NPY)-positive but not proopio-

melanocortin (POMC)-positive cells. Finally, these actions of enteric glucose were reduced in diabetic mice fed a high-fat, carbohydrate-free diet.

RESEARCH DESIGN AND METHODS

Twelve-week-old C57BL6/J (Janvier, St Berthevin, France), GLP-1Rc knock-out (in a C57BL6/J background, from our colony), and NPY–green fluorescent protein (GFP) (in a C57BL6/J background, a gift from J. Friedman) male mice were housed in a controlled environment (inverted 12-h daylight cycle with lights off from 10:00 A.M. to 10:00 P.M.) with free access to food and water. Mice were fed a normal chow (A04; Unité Aliment Rationnel, Villemoisson sur Orge, France) or a high-fat, carbohydrate-free diet for a period of 4 weeks. The diet contained 72% fat (corn oil and lard), 28% protein, and <1% carbohydrate, as energy content. This diet has been shown to induce diabetes before an increase in body weight (23). All animal experimental procedures were approved by the Rangueil Hospital Committee of the Rangueil Hospital (Toulouse, France).

Surgical procedures

Indwelling intragastric catheter. Under anesthesia (ketamine/xylazine, 100 and 10 mg/kg i.p., respectively), a catheter was inserted into the stomach. Briefly, a 4-mm laparotomy was performed on the left side of the abdomen, and the stomach was gently extracted. One centimeter of the teflon catheter was inserted into the stomach and secured by surgical glue (Histoacryl; 3M Health Care, St. Paul, MN). The other extremity of the catheter was tunneled under the skin and exteriorized at the back of the neck.

Indwelling intracerebroventricular catheter. Under similar anesthesia, a 1-cm midline incision was made across the top of the skull, the animal was placed on a stereotaxic apparatus, and the periosteum cleaned as described previously (24). A hole, 1 mm in diameter, was made 0.1 mm lateral, 0.22 mm anteroposterior from the bregma, and 1.7 mm deep; through it, a cannulae was inserted to reach the lateral ventricle. Two supporting screws were placed bilaterally, one in the posterior quadrants of the skull and the other one in the anterior part of the skull, and secured in place with acrylic dental cement (Magasin Général Dentaire, Paris, France). The cannulae (Alzet, Lupertino, CA) was filled with artificial cerebral fluid (Harvard Apparatus, Les Ulis, France) and connected to a sealed Tygon catheter (Norton, Akron, OH). To determine the role of brain GLP-1 signaling, we infused into the lateral ventricle of the brain the GLP-1Rc antagonist Exendin 9-39 (Ex9; 0.5 pmol · kg^{-1} · min^{-1}; Bachem), or artificial cerebrospinal fluid (Harvard Apparatus) as control, at a rate of 12 μl/h, as previously described (23).

Indwelling intrafemoral catheter. Under similar anesthesia, a catheter was inserted into the femoral vein as described previously (25).

All mice were allowed to recover for 3 weeks after surgery before undergoing experimental infusions. The mice that did not regain their presurgical body weight were not used for subsequent studies.

Training period. Because the nervous system is highly dependent on perception of environmental stress, 3 weeks after surgery, the mice were trained for 5 consecutive days with repeated daily handling, before undergoing the final experiments (Fig. 1A). Briefly, during the training period, mice were connected to the infusion system at 9:00 A.M. each morning. While remaining in their cage bedding, the mice were left untouched inside the cage in a quiet environment with free access to water. Six hours later, the infusion pumps were turned on. During the training period, mice were infused daily with a bolus of water (100 μl during 10 min).

On the 3rd day of the training period, the correct catheter implantation was verified by infusing a rate of glucose high enough to ensure hyperglycemia (30 mg · kg^{-1} · min^{-1}). The mice were left inside their cage, and glycemia was followed every 10 min for 2 h by gentle sampling of a drop of blood (<5 μl) from the tip of the tail vein. Less than 60 μl blood was sampled. Mice with a blood glucose >9 mmol/l after glucose infusion were considered to demonstrate proper catheter placement and used for further experiments.

Experimental design for the assessment of basal whole-body glucose turnover rates: protocol 1 (Fig. 1A). The determination of glucose turnover rate requires that a glucose tracer be infused, reaching a steady-state concentration into the blood. To respect this principle, a first set of mice was continuously infused with glucose at a rate of 10 mg · kg^{-1} · min^{-1} or water into the stomach after 6 h of fasting. Simultaneously, a tracer dose of D-[3-^{3}H]glucose (Perkin Elmer, Boston, MA) was continuously infused through the femoral vein at a rate of 10 μCi · kg^{-1} · min^{-1}. Plasma D-[3-^{3}H]glucose enrichment was determined from total blood (5 μl) collected at the tip of the tail vein every 10 min of the last hour of infusion. This represents 30 μl blood—hence, a small volume. In previous sets of identical experiments, hematocrit was assessed before and after the infusion. The values were similar before (39 ± 1%) and at completion (37 ± 2%) of the infusion, showing the lack of hemodilution because of the infusion and sampling procedures.

The sampled blood was then immediately deproteinized by a Zn(OH)$_2$ precipitate as previously described (26). After centrifugation, an aliquot of the supernatant was evaporated to dryness to determine the radioactivity corresponding to D-[3-^{3}H]glucose. In a second aliquot of the same supernatant, glucose concentration was assessed by a glucose oxidase method as described previously (26).

At completion of the infusion, the liver and hindlimb muscles were quickly harvested and frozen until assay.

Experimental design to determine c-Fos expression pattern: protocol 2 (Fig. 1A). On the 6th day, to assess neuronal c-Fos expression in mice without inducing systemic hyperglycemia, animals were infused with a low rate of glucose (10 mg · kg^{-1} · min^{-1} for 10 min only) or water into the stomach (total volume 100 μl over 10 min) after 6 h of fasting. This rate represents one-half of the endogenous glucose production over a short period of time, which allows for the stimulation of the enteric sensor without inducing systemic hyperglycemia. No handling of the mouse was performed until the brain was fixed 2 h later as follows. Under anesthesia, a cannulae was implanted into the left ventricle to ensure the delivery of an ice-cold PBS (0.1 mol/l, pH 7.4) infusion followed by a 4% picric acid buffer and 4% formaldehyde infusion. The brain was removed from the skull, postfixed with the formaldehyde buffer, cryoprotected one night in 20% sucrose, sectioned, and stained for immunohistochemistry.

Immunohistochemistry. Thirty-five-micrometer–thick slices of frozen brain coronal sections were used to perform immunohistochemical detection of c-Fos–expressing cells. Free-floating brain sections were incubated overnight with a rabbit polyclonal c-Fos antibody (dilution 1:10,000; Ab-5; Oncogene, San Diego, CA) at 4°C. Sections were rinsed in PBS and incubated for 1 h at room temperature with a secondary biotinylated goat anti-rabbit antibody diluted 1:2,000 (The Jackson Laboratories, West Grove, PA). Sections were incubated for 45 min with a streptavidin-peroxidase complex (The Jackson Laboratories) at room temperature. After rinsing in PBS, brain sections were incubated with nickel-peroxidase substrate kit solution (Vector Laboratories, Orton Southgate, Peterborough, U.K.) at room temperature.

The number of c-Fos–positive cells was determined in the NTS, ARC, ventromedian hypothalamus (VMH), and dorsomedian hypothalamus (DMN), quantified using Visilog 6 software (Neosis, Les Ulis, France), and counted in one of two counterstained sections separated by 35 μm (Fig. 1B).

Colocalization of c-Fos–, NPY-, and POMC-positive cells. Free-floating sections at thickness of 35 μm in the ARC of the hypothalamus were processed for the colocalization of c-Fos, NPY, and POMC. In the first set of experiments, POMC and c-Fos were colocalized by immunofluorescence. After overnight incubation with a rabbit polyclonal anti–c-Fos primary antibody (1:1,000; Santa Cruz Biotechnology, Santa Cruz, CA) at room temperature, sections were rinsed and incubated for 1 h with biotinylated goat anti-rabbit IgG (1:200; Jackson ImmunoResearch) and sequentially with avidin-biotin-horseradish peroxidase for 1 h (1:500; Vector Laboratories). Signals were amplified with biotinylated tyramide for 10 min (1:250; Tyramide Signal Amplification; NEN, Boston, MA) before incubation with Cy3-conjugated streptavidin antibody (1:200; Jackson ImmunoResearch) for 45 min. For double labeling with POMC, sections were subsequently incubated with a rabbit polyclonal anti-POMC primary antibody (1:1,000) overnight at room temperature and then with Alexa 488-conjugated anti-rabbit antibody (1:100; Molecular Probes) for 45 min. Each primary antibody was tested separately, and immunohistochemical controls were performed by omitting the primary antibody.

In a second set of experiments, NPY and c-Fos were colocalized by immunohistochemistry because immunofluorescence was not successful. Briefly, 35-μm slices were incubated for 6 h with goat serum (10%) at room temperature in Tris-buffered saline, pH 7.6. The primary antibody against c-Fos (1/20,000; Calbiochem) was incubated at room temperature overnight. The slides were rinsed and treated with H$_2$O$_2$ (1%) for 30 min. The slides were then incubated with the secondary antibody (1/200) for 2 h at room temperature. The secondary antibody was revealed using streptavidin peroxidase coupled with diaminobenzidine (DAB) nickel staining (Calbiochem). The next day, a primary antibody against GFP was incubated (1/200; Serotech) with the slides at room temperature, rinsed, incubated with H$_2$O$_2$ as above, and incubated with the secondary biotinylated antibody (1/1,000; Jackson ImmunoResearch) for 2 h at room temperature. The slides were rinsed, and the labeling was revealed using streptavidin peroxidase and DAB-only staining (to discriminate from c-Fos labeling). NPY- and c-Fos–positive cells were counted manually by two different experimenters. The percentage of colocalization was calculated by dividing the number of c-Fos– and NPY– co-positive cells by the number of NPY-positive cells.

Signals for c-Fos and POMC were captured using a fluorescence microscope (Axioplan 2 Imaging; Carl Zeiss). Colocalization of c-Fos and POMC was determined by merging the individual signals of c-Fos and POMC with Adobe Photoshop 7.0 after the number of c-Fos– and POMC-positive cells was
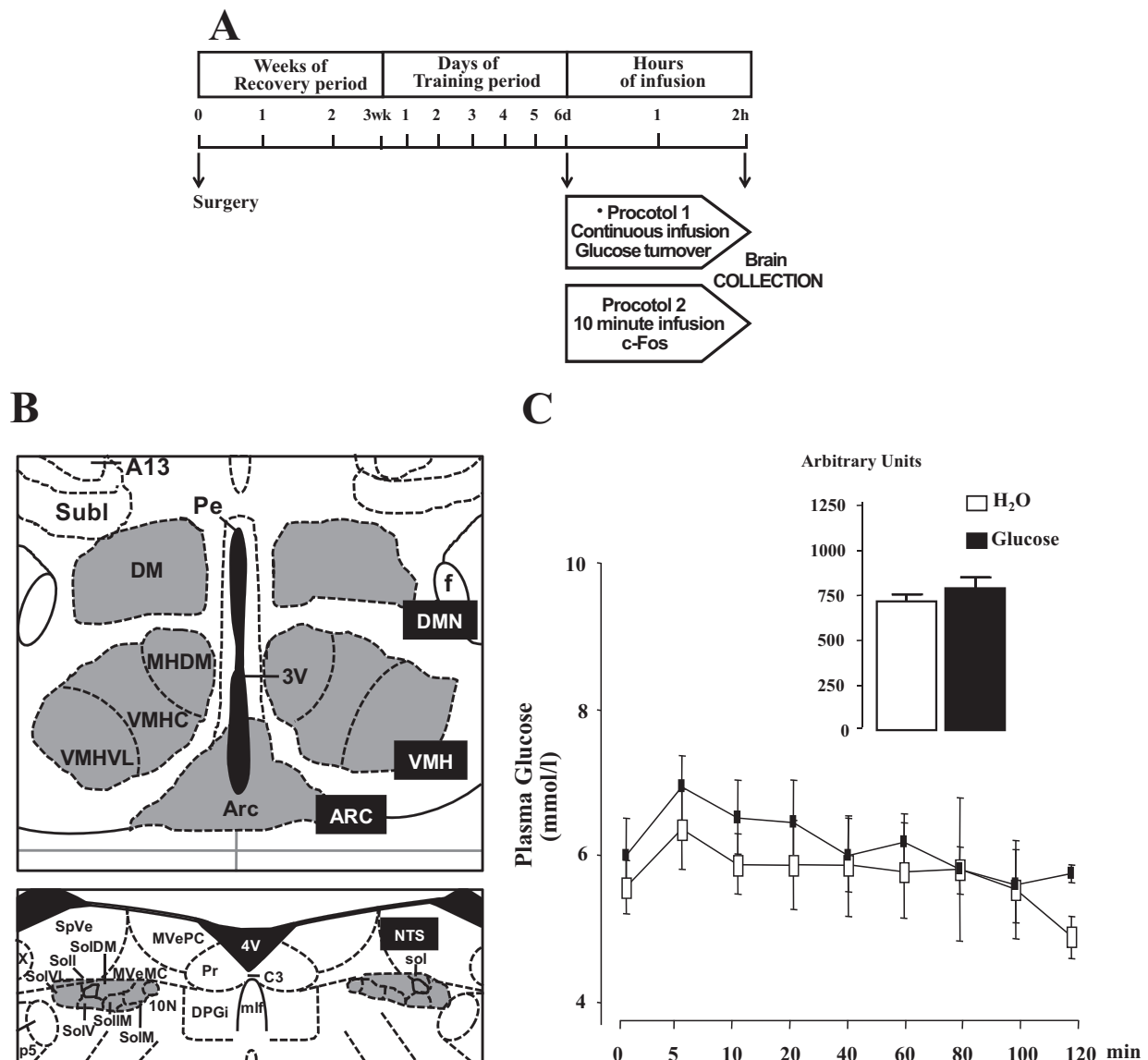
FIG. 1. *A*: Experimental design to analyze the effect of an intragastric glucose infusion. Mice bearing intragastric, femoral, and intracerebroventricular catheters underwent infusions after the surgery recovery period. On days 1, 2, 4, and 5 of the training period, mice were trained to the intragastric water infusion. On day 3, an intragastric glucose infusion (30 mg · kg^{-1} · min^{-1}) was performed, and those mice developing immediate hyperglycemia demonstrated a correct intragastric catheter implantation and were studied on day 6 when they underwent an intragastric glucose or water infusion after 6 h of fasting. Two protocols were set up. In protocol 1, glucose turnover was assessed and the mice underwent a continuous intragastric glucose infusion for 2 h. In protocol 2, the mice underwent a 10-min intragastric glucose or water infusion, and 2 h later, the brain was fixed in vivo for histological studies. *B*: Schematic representation in gray of brain areas analyzed to quantify the number of c-Fos–positive cells (37). *C*: Glycemic profiles (mmol/l) in mice infused with glucose (■) or saline (□). The *inset* represents the corresponding AUC (arbitrary units). No differences were noticed.

separately counted. The percentage of colocalization was calculated by dividing the number of c-Fos– and POMC–co-positive cells by the number of POMC-positive cells.

Plasma insulin and GLP-1 (7-36) concentrations. In a fourth set of experiments to determine portal plasma parameters, portal blood was collected just after completion of the 10-min intragastric injection in tubes containing 10 μl/ml DPP-IV inhibitor (Linco Research, St. Charles, MO). At completion of the infusions, the mice were rapidly anesthetized with ketamine/xylazine, the portal vein was surgically exposed, and a sample of portal blood (200 μl) was collected. Plasma was immediately sampled and frozen for further analyses.

Plasma biochemical analyses. Portal plasma glucose concentration was measured using an enzymatic glucose oxidase procedure (Elitech Sopachem, Wageningen, The Netherlands). Portal and systemic plasma insulin levels were measured by ELISA (Ultrasensitive Mouse Insulin-High Range Mouse Insulin ELISA kit; Mercodia, Uppsala, Sweden). Portal plasma GLP-1 (7-36) amide concentrations were measured using an ELISA method (GLP-1 active ELISA kit; Linco Research) as previously described (27).

Determinations of liver and muscle glycogen synthesis rates. Liver and muscle glycogen synthesis rates were determined by extracting total glycogen, which includes unlabeled glycogen and [3-^{3}H]glycogen, with 6% (w/v) perchloric acid and precipitating glycogen with ethanol as previously described (24). Briefly, 100 mg hindlimb muscle or liver were homogenized in 10 volumes of perchloric acid and spun down to eliminate nonhomogenized particles. The supernatant was precipitated with 15 volumes of ice-cold absolute ethanol overnight. The glycogen was precipitated by an overnight exposure at −20°C and recovered by centrifugation. The precipitating procedure was performed twice to ensure the elimination of soluble D-[3-^{3}H]glucose. The precipitated radioactive glycogen was then dissolved in distilled water, and the radioactivity was counted in the presence of scintillation buffer.

Calculations and statistical analysis. Calculation of glucose turnover was made from parameters obtained during the last 60 min of the infusions under steady-state conditions as described previously (24). Briefly, the D-[3-^{3}H]glucose specific activity was calculated by dividing the D-[3-^{3}H]glucose enrichment by the plasma glucose concentration. The whole-body glucose turnover rate was calculated by dividing the rate of D-[3-^{3}H]glucose infusion by the

D-[3-³H]glucose plasma specific activity. Endogenous glucose production rate cannot be calculated because our experimental procedure does not allow the determination of the enteric glucose absorption or net hepatic glucose uptake rates. Since the unlabeled glucose is not infused into the same compartment as the tritiated glucose, the turnover rate cannot take into account the rate of hepatic glucose production. Consequently, the whole-body glucose utilization rate cannot be the sum of endogenous glucose production and exogenous glucose infusion rates. Similar reasoning and calculations were discussed previously (4,14,28).

The whole-body glycolytic flux was calculated from the [³H]₂O accumulated in the plasma during the last hour of the infusions. The whole-body glycogen synthesis rate was calculated by subtracting the glycolytic flux from the glucose turnover rate. For each mouse, the mean values have been calculated and then averaged with values from mice from the same group. The muscle and liver glycogen synthesis rates have been calculated by dividing the D-[3-³H]glucose muscle glycogen content by the duration of the infusion and by the D-[3-³H]glucose specific activity in the blood. Hence, the value should be considered an index of the glycogen synthesis rate. Mice showing variations of the steady-state D-[3-³H]glucose specific activity >15% during this time period were excluded from the study. Results are presented as means ± SE. Statistical significance of differences was analyzed by using Student's *t* test for unpaired bilaterally distributed values of unequal variance. Area under the curve (AUC) was calculated using the trapezoid rule. Correlations between parameters were assessed by Pearson's correlation test using GraphPad Prism version 4.00 for Windows (GraphPad Software, San Diego, CA; www.graphpad.com). Values were considered different when $P < 0.05$.

RESULTS

Effect of intragastric glucose infusion on plasma parameters. This first set of mice was infused with glucose into the stomach at a rate of one-half of the endogenous glucose production rate of $(10 \text{ mg} \cdot \text{kg}^{-1} \cdot \text{min}^{-1})$ for 2 h (Fig. 1*A*). This experimental procedure selectively activates the gut-glucose sensor system without producing systemic hyperglycemia. It could also activate the hepatoportal glucose sensor, although to a much lower extent, because the portal glycemia rose modestly from 6.3 ± 0.2 to 7.1 ± 0.3 mmol/l, $P < 0.05$, in water- and glucose-infused mice, respectively. Similarly, systemic glycemia (tail vein) was assessed every 5 min for the first 20 min and then every 20 min during the following 2 h in this set of mice only. Peripheral glycemia varied between 6 and ~7 mmol/l in both water and low glucose infusion rate groups for the first 40 min (Fig. 1*C*) and then progressively stabilized between 5 and 6 mmol/l until completion of the infusions. Consequently, the AUCs of glycemic profiles were similar between glucose- and water-infused mice (Fig. 1*C*). In addition, in different sets of animals, the peritoneal infusion of glucose did not change portal glucose concentration (6.61 ± 0.92 vs. 5.91 ± 1.02 mmol/l in saline and intraperitoneal glucose, respectively). Similarly, GLP-1 concentration remained unchanged (7.43 ± 0.81 vs. 5.45 ± 0.39 pmol/l in saline and intraperitoneal glucose, respectively).

These results validate the procedure for predominant activation of enteric glucose sensors because peripheral glycemia was only very moderately and transiently increased. This procedure can hence facilitate analysis of the roles of enteric versus systemic glucose sensors.

In a different set of mice, plasma insulin concentrations were assessed before and 4 and 15 min after the beginning of the continuous intragastric glucose infusion procedure. Systemic plasma insulin concentrations were unchanged under these conditions: 66 ± 6, 72 ± 6, and 72 ± 30 versus 55 ± 6, 85 ± 18, and 90 ± 30 pmol/l, before and at 4 and 15 min in water- and glucose-infused mice, respectively. However, portal vein insulin concentration was 264 ± 96 versus 546 ± 72 pmol/l in water- and glucose-infused mice, respectively. It is noteworthy that despite the increased portal insulin concentration, no change in systemic insulin concentration was noticed, suggesting that the liver had a major role in insulin clearance. Conversely, portal GLP-1 concentrations were unchanged by the enteric glucose infusion (6.54 ± 0.11 vs. 6.79 ± 0.27 pmol/l in water- and glucose-infused mice, respectively). To delineate the role of brain GLP-1 signaling in the control of plasma parameters, Ex9 was infused into the brain, and glucose or water was infused into the stomach. Portal glucose (6.6 ± 0.6 vs. 6.1 ± 0.5 mmol/l), insulin (106.4 ± 68.3 vs. 98.5 ± 29.8 pmol/l), and GLP-1 (5.6 ± 0.3 vs. 4.4 ± 0.2 pmol/l) concentrations were similar between mice infused for 10 min with glucose or water into the stomach, respectively. We performed the same analysis in mice fed a high-fat, carbohydrate-free diet and showed that portal glucose (7.2 ± 0.6 vs. 6.2 ± 0.7 mmol/l), insulin (134.3 ± 45.9 vs. 129.8 ± 48.2 pmol/l), and GLP-1 (5.5 ± 0.2 vs. 5.0 ± 0.3 pmol/l) remained unchanged in glucose- and water-infused mice, respectively. This suggests that the diabetic state has affected the enteric glucose sensor for the control of plasma parameters as well.

Effect of intragastric glucose infusion on glucose turnover rates. To assess the role of the enteric glucose sensor on the control of glucose fate, a 2-h low-rate intragastric glucose infusion was performed in conscious, free-moving mice. Whole-body glucose turnover rate was elevated by the glucose infusion to 160% of control values (Fig. 2*A*). Whole-body glycogen synthesis and glycolytic rates were increased to the same extent (Fig. 2*A*). The increased glucose utilization rate was accompanied by a twofold augmentation of muscle glycogen synthesis in the low-rate glucose-infused mice, whereas liver glycogen synthesis rate was unchanged (Fig. 2*B* and *C*). It is noteworthy that the liver glycogen synthesis rate is very low in GLP-1Rc knockout mice, which could be due to the rather hypoinsulinemic state of these mutant mice.

Effect of intragastric glucose infusion on c-Fos expression pattern in the brain. To determine whether the effect of the intragastric glucose infusion on the control of glucose fate was associated with activation of specific neuronal populations, we quantified the number of c-Fos–positive cells in the NTS, ARC, VMH, and DMN (Fig. 1*B*) 2 h after an intragastric infusion of water or glucose. In the NTS, the number of c-Fos–positive cells significantly increased by ~four- to fivefold after glucose infusion. In contrast, the number of c-Fos–positive cells was reduced in the ARC, VMH, and DMN hypothalamic nuclei by 75, 30, and 35%, respectively (Fig. 3*A–C*).

To assess the putative confounding effects of changes in osmotic pressure during the intragastric infusion experiment, we studied mice after intragastric infusion with NaCl (0.9%) (305 vs. 185 mOsmol/l in NaCl and the glucose solution, respectively). No difference in c-Fos expression pattern was noted between water- and NaCl-infused mice (not shown). Hence, because water is considered a naturally ingested solution, all control groups were subsequently infused with water. In addition, the procedure aims at minimizing gastric distension by infusing the glucose solution for 10 min in a small volume of 100 μl. The same conditions were used in water-infused mice.

Effect of GLP-1Rc blockade on glucose turnover rates during intragastric glucose infusion. To study the role of the GLP-1Rc on the control of whole-body glucose fluxes in response to activation of the gut-glucose sensor, we infused glucose in the stomach for 2 h in GLP-1Rc knockout mice (protocol 1; Fig. 1*A*). In these mice, whole-
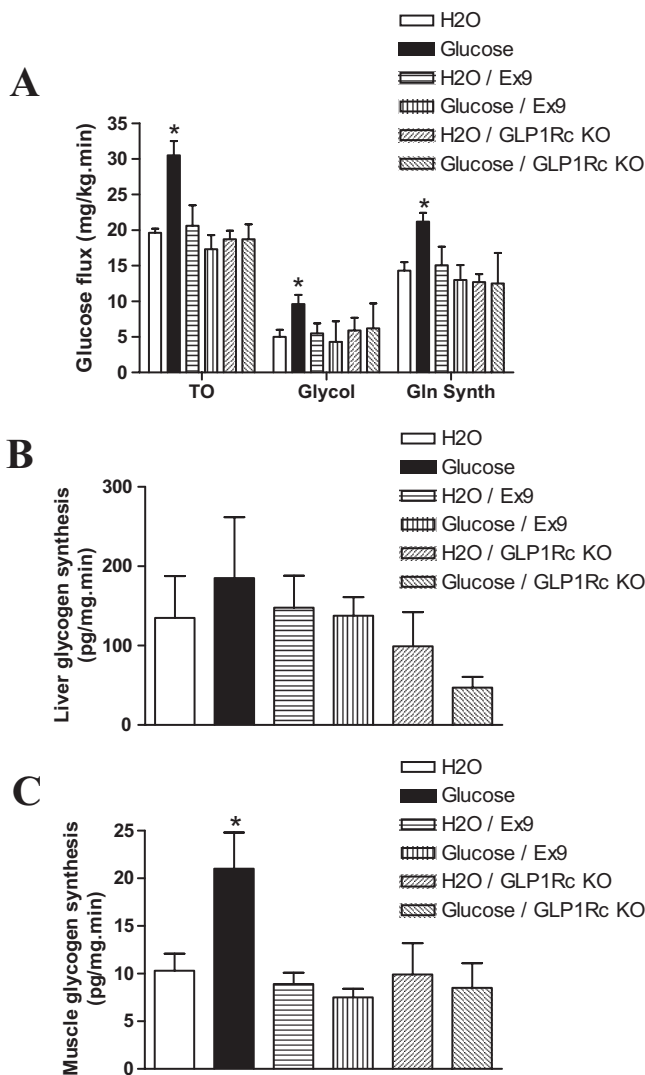
A

B

C

FIG. 2. Glucose turnover and glycogen synthesis rates. *A*: Whole-body glucose turnover, glycolysis, and glycogen synthesis rates ($mg \cdot kg^{-1} \cdot min^{-1}$). Glycogen synthesis rates ($pg \cdot mg^{-1} \cdot min^{-1}$) in liver (*B*) and muscle (*C*) were assessed after a 2-h water or glucose intragastric infusion (protocol 1) in wild-type and GLP-1Rc knockout (GLP-1Rc KO) mice (see protocol 1 in Fig. 1). A subset of wild-type mice was infused simultaneously with Ex9 into the brain (Ex9). Five to nine mice per group were studied. *Statistically different from water-infused control mice when *P* < 0.05.

A

B

C

FIG. 3. Pattern of c-Fos–positive cells after an intragastric glucose infusion. The number of c-Fos–positive cells was quantified in the NTS (*A*) and ARC, VMH, and DMN nuclei (*B*) (as described in Fig. 1*B*) of C57BL/6 mice infused with water (□) or glucose (■) for 10 min (see protocol 2 in Fig. 1). *C*: Representative staining of c-Fos–expressing cells in each nuclei and condition. Eight mice per group were studied. *Statistically different from water-infused control mice when *P* < 0.05. **Statistically different from water-infused control mice when *P* < 0.01.

body glucose turnover, glycolysis, and glycogen synthesis rates were no longer increased by gastric glucose infusion (Fig. 2*A*). However, the GLP-1Rc knockout mice were not hyperglycemic. Our experimental design cannot allow for the precise determination of hepatic glucose production because glucose was infused into the stomach, and therefore no interpretation can be drawn with regard to the role of the liver. This would require the use of different sets of tracers not applicable to mouse infusion procedures, as discussed previously (4).

Because GLP-1Rcs are also present in brain, the elimination of the enteric glucose signal in GLP-1Rc knockout mice does not permit precise localization of the specific tissues important for the GLP-1Rc–dependent control of the enteric glucose sensor. To investigate the importance of brain GLP-1 signaling, we infused the GLP-1Rc antagonist Ex9 into the brain of wild-type mice while the glucose was simultaneously infused into the stomach. Central Ex9 completely eliminated the changes in glucose turnover
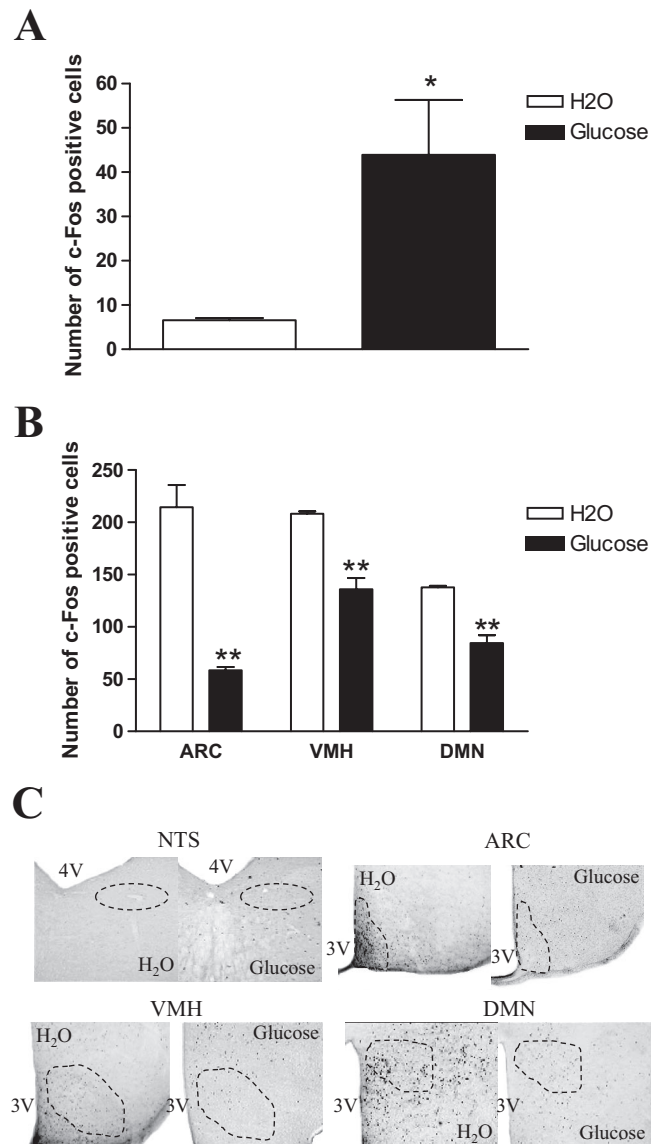
rate, glycolysis, and muscle glycogen synthesis, consistent with findings using GLP-1Rc knockout mice (Fig. 2*A*–*C*). Hence, GLP-1Rc activation in the brain is necessary for transduction of the enteric glucose signal.

Effect of GLP-1Rc blockade on c-Fos expression pattern during intragastric glucose infusion. We then assessed whether activation of the GLP-1Rc was essential for regulation of the neural c-Fos expression pattern observed in response to the activation of enteric glucose sensor. Intragastric glucose infusion failed to increase the number of c-Fos–positive cells in the NTS of GLP-1Rc knockout mice (Fig. 4*A*). Similarly, no effect of enteric glucose on c-Fos expression was observed in hypothalamic nuclei (Fig. 4*B*).

Colocalization of c-Fos–positive cells with POMC- or NPY-positive cells in the ARC. We then identified the population of neuronal cells targeted into the brain by the
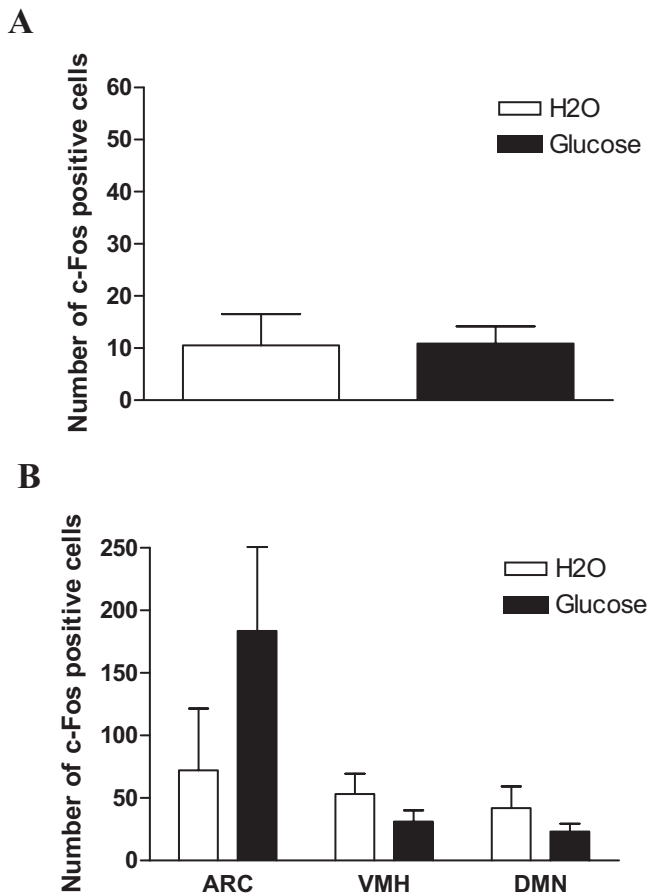
A

B

FIG. 4. Pattern of c-Fos–positive cells after an intragastric glucose infusion in GLP-1Rc knockout mice. The number of c-Fos–expressing cells was quantified in the NTS (*A*) and ARC, VMH, and DMN nuclei (*B*) of GLP-1Rc knockout mice (as described in Fig. 1*B*) infused with water (□) or glucose (■). Five mice per group were studied. No differences were noted between groups.

enteric glucose signal. Only a relatively small portion (7%) of all POMC-positive cells was colocalized with c-Fos–positive cells, and there was no significant difference of number of c-Fos– and POMC–co-positive cells between water- and glucose-infused mice (Fig. 5*A–C*). In contrast, ~25% of NPY-positive cells expressed c-Fos, and this proportion decreased to 10% in response to enteric glucose (Fig. 5*D–F*).

High-fat, carbohydrate-free diet impairs the glucose-dependent enteric signal. We next assessed the impact of high-fat, carbohydrate-free diet on c-Fos expression pattern in the brain in response to enteric glucose. Fasted glycemia was 7.9 ± 0.6 versus 10.6 ± 0.2 mmol/l in control mice and mice fed a high-fat, carbohydrate-free diet, respectively ($P < 0.05$ when comparing both groups). All mice studied were glucose intolerant as determined after an intraperitoneal glucose challenge. The AUCs of the glucose profiles were 3,329 and 4,950 mmol · l^{-1} · min^{-1} in control mice and mice fed a high-fat, carbohydrate-free diet, respectively ($P < 0.05$ when comparing both groups). We have previously described the main diabetic features of this animal model (25). In the diabetic mice, enteric glucose did not increase whole-body glucose utilization rate (Fig. 6*C*) or modify the c-Fos expression pattern in the NTS or ARC (Fig. 6*A* and *B*).

DISCUSSION

The present study demonstrates the following: *1*) the enteric glucose sensor system controls whole-body glucose utilization, particularly muscle glycogen synthesis; *2*) this sensor results in changes in neuronal activity in both hypothalamus and brain stem connected to NPY-positive cells; *3*) this sensor requires activation of brain GLP-1Rc; and *4*) the "gut-brain-muscle" axis is altered after high-fat feeding.

Enteric glucose sensor system controls whole-body glucose utilization and muscle glycogen synthesis. During a meal, glucose is absorbed by the intestine and either stored or oxidized by tissues. In the present study, we assessed the role of enteric glucose sensors on whole-body glucose fluxes and glycogen synthesis. To selectively activate the enteric sensor, glucose was infused into the stomach at a very low rate that did not induce systemic hyperglycemia. Under these conditions, whole-body glucose utilization and muscle glycogen synthesis were increased, showing a functional connection between the enteric area, which includes the portal vein, and peripheral tissues (Fig. 7). It is noteworthy that although we did not notice a large increase in the portal glucose concentration over the first 10 min after the glucose administration, we cannot rule out that the portal sensor was not activated as well. In favor of a role of intestinal glucose sensing, it has recently been shown that the sweet-taste receptor subunit T1R3 and the taste G-protein gustducin are expressed in enteroendocrine cells and underlie intestinal sugar sensing and regulation of SGLT1 mRNA and protein (29). We could hypothesize that this taste receptor would be part of the enteric glucose sensor. Its activation seems to be mainly dependent on glucose itself. However, we cannot rule out that the small rise in portal insulin concentration would have contributed to the generation of the enteric signal toward the brain. We previously reported that 2 min after an oral glucose challenge, there was a rapid increase in insulin secretion that was dependent on the GLP-1Rc located into the portal vein (30). However, in the set of data, the glucose challenge value was much lower than the classic oral glucose tolerance test. This led to a smaller increase in portal insulin concentration that was not reaching the systemic blood.

Our present data suggest that the enteric and brain sensors generate opposite signals for the control of peripheral glucose metabolism (Fig. 7). This hypothesis is supported by previous data demonstrating that glucose infusion directly into the brain, to activate the corresponding sensor, reduced peripheral glucose utilization (24), whereas in the present study, the activation of the enteric sensor increases peripheral glucose utilization. Our findings show that within minutes of administration into the stomach, glucose can alter neuronal activity and facilitate peripheral tissues to store glucose. This conclusion is also supported by data from the literature showing that a low enteric glucose infusion in the rat rapidly increases pancreatic blood flow, preparing the islets for insulin secretion through a mechanism requiring the vagus nerve (31). In addition to the role of the autonomic nervous system, functional GLP-1Rcs represent an important component of the enteric glucose sensor. GLP-1 is released into the portal vein and controls the firing rate of the vagus nerve (32) and the hepatoportal sensor system, leading to an increased whole-body glucose utilization rate (14). However, our current data show
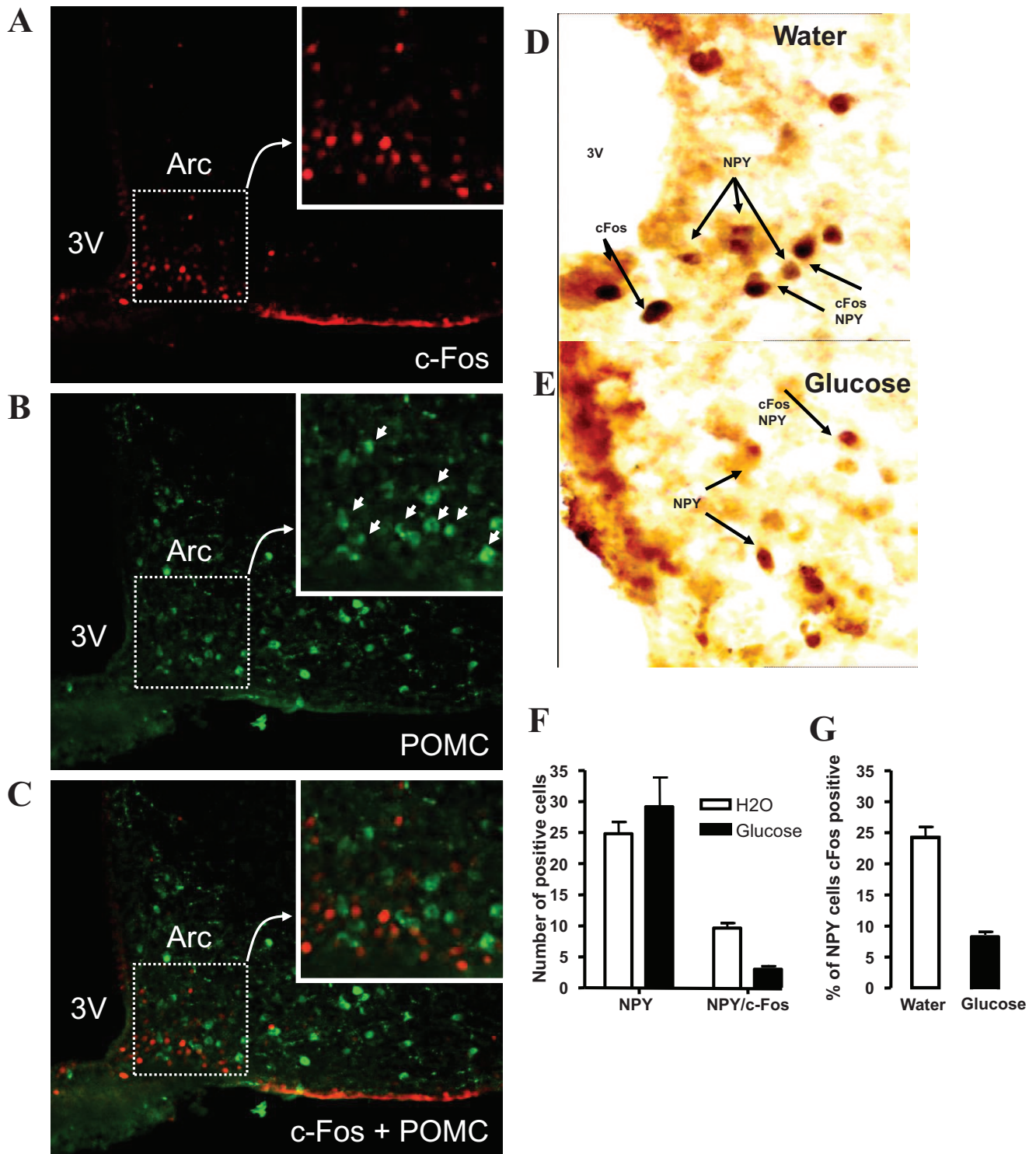
FIG. 5. Pattern of c-Fos/POMC– and c-Fos/NPY–positive cells after an intragastric water or glucose infusion. c-Fos/POMC–positive cells were quantified in the ARC. Representative figures of c-Fos–positive cells (A) and POMC-positive cells (B) in the ARC. ARC was magnified. The POMC-positive cells showing clear staining in cytoplasm are indicated by white arrows. C: Representative figure of c-Fos/POMC–positive cells showing that POMC-positive cells were not colocalized with c-Fos in the magnified field. c-Fos/NPY–positive cells was quantified in the ARC. D and E: Immunohistochemical representation of cFos and NPY and NPY/cFos-positive cells, as indicated by arrows, in mice infused with water or glucose. F and G: Quantification of NPY and NPY/c-Fos-positive cells in mice infused with water (□) or glucose (■). Five to six mice per group were studied. (Please see http://dx.doi.org/10.2337/db07-1788 for a high-quality digital representation of this figure.)

that the portal vein GLP-1 (7-36) amide concentration remained unchanged 10 min after the initiation of intragastric glucose infusion, hence it is unlikely that portal GLP-1 represents the gut-glucose signal.

Brain stem and hypothalamic nuclei are differentially regulated by enteric glucose. The first synapse of vagal afferents are in caudal brain stem nuclei (6), where we observed increased numbers of c-Fos–expressing cells in
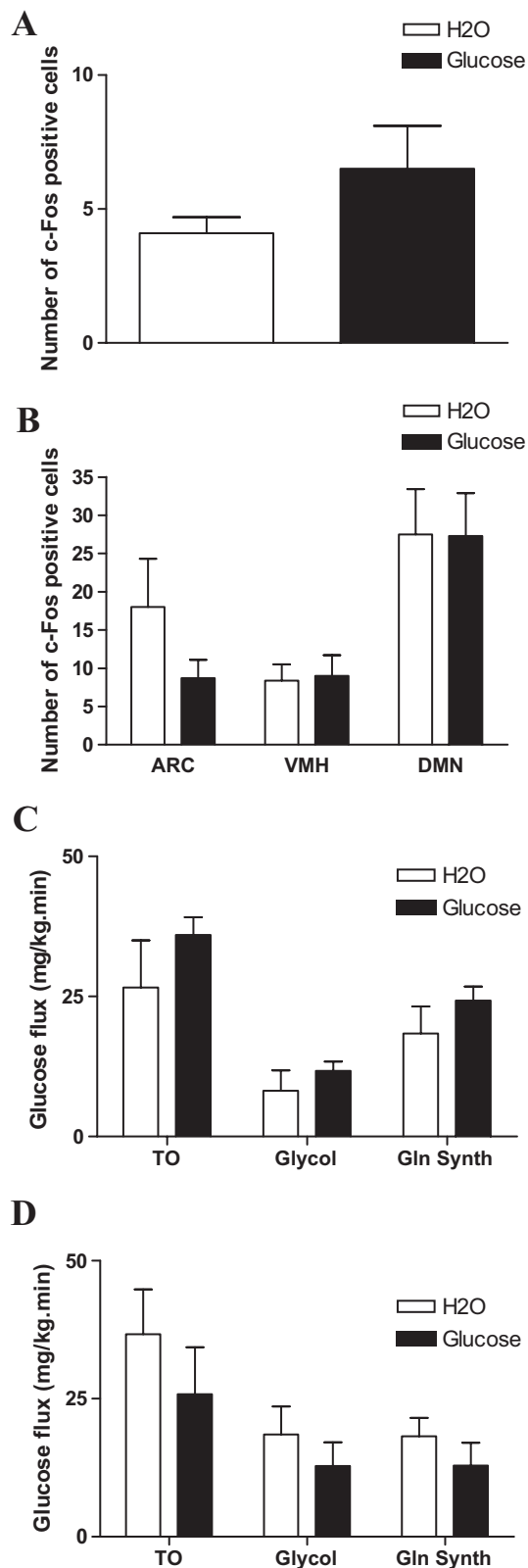
FIG. 7. Schematic representation of the role of GLP-1 in the brain as a master switch for the control of glucose fate. *1*) Enteric sensors are the first site for glucose detection after an oral glucose load. They send a neural signal to the NTS. *2*) Subsequently, the NTS sends a signal toward the hypothalamus, including GLP-1. The enteric signal triggers NPY-positive cells. *3*) GLP-1–sensitive cells send a new signal, of unknown origin, toward peripheral tissues, i.e., muscles, to prepare cells to use glucose. *4*) The brain would detect glucose. *5*) Subsequently, a signal opposite to the one sent by the enteric glucose detector would be sent by the brain to the muscle, as previously described (23). Importantly, the enteric glucose signal is impaired during diabetes.

FIG. 6. Pattern of c-Fos–positive cells and glucose utilization rates after an intragastric glucose infusion in high-fat diet–fed diabetic mice. The number of c-Fos–expressing cells was quantified in the NTS (*A*) and ARC, VMH, and DMN nuclei (*B*) of mice fed a high-fat, carbohydrate-free diet infused with water (□) or glucose (■). Five mice per group were studied. Glucose flux ($mg \cdot kg^{-1} \cdot min^{-1}$) was studied after 1 week (*C*) or 1 month (*D*) of high-fat, carbohydrate-free diet. TO, turnover; Glycol, glycolysis; and Gln Synth, glycogen synthesis. For all parameters, no difference was noted between groups.
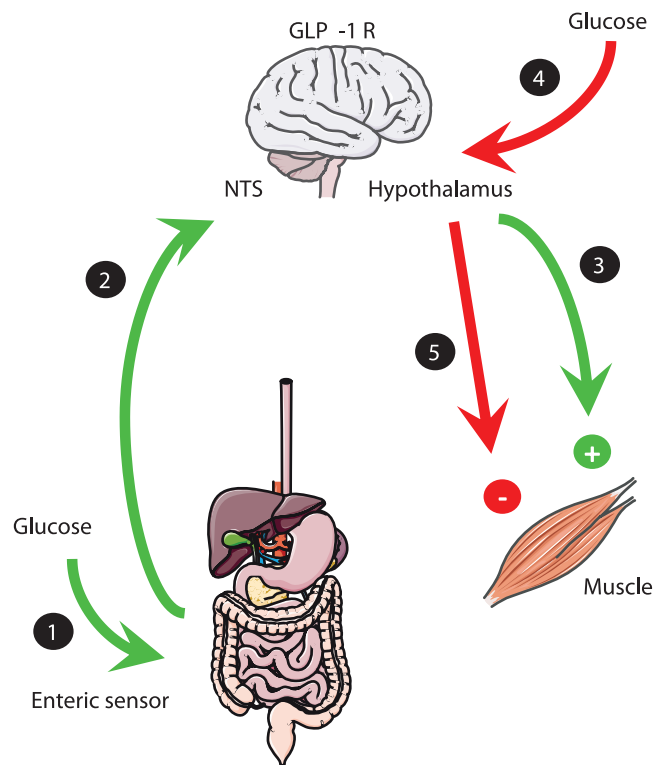
mice receiving intragastric glucose infusions. Interestingly, the pattern was quite different in hypothalamic nuclei. Intragastric glucose infusion reduced the number of c-Fos–expressing cells in the ARC, VMH, and DMN. Interestingly, data from our group showed that an intragastric glucose infusion high enough to induce systemic hyperglycemia increased the number of c-Fos–positive cells in hypothalamic nuclei (unpublished observations). Similar data were previously reported by others and showed that a direct glucose infusion in the brain through the carotid artery increased the number of c-Fos– expressing cells in hypothalamic nuclei, notably, the arcuate, paraventricular, and ventromedian nuclei (33). Together, the signals generated by the enteric sensor are opposite to those generated by hyperglycemia in the brain (Fig. 7).

The enteric glucose sensor system sends signals to peripheral tissues via a mechanism that requires a functional brain GLP-1Rc. In response to a low-rate intragastric glucose infusion, the c-Fos expression pattern in GLP-1Rc knockout mice was different from that detected in wild-type mice. The number of c-Fos–positive cells was not increased in response to intragastric glucose in the NTS of GLP-1 Rc knockout mice when compared with wild-type controls. Similarly, no increased muscle glycogen synthesis was observed in wild-type mice infused with glucose into the stomach when the GLP-1Rc antagonist Ex9 was simultaneously infused into the brain. This suggests that GLP-1 could be released in the brain in

response to gastric glucose. In the absence of peripheral hyperglycemia and hyperinsulinemia, the enteric signal would increase peripheral glucose metabolism (Fig. 7). Taken together, our current data suggest that enteric glucose activates a GLP-1Rc–dependent signal in the brain to control peripheral glucose metabolism. GLP-1–producing neurons are found largely in the NTS, where they project to a number of hypothalamic nuclei (15,34), and therefore may provide a key link between brainstem and hypothalamic neuronal populations regulated by gastric glucose infusion.

The enteric glucose signal triggers NPY neurons in the ARC. We determined that 25% of NPY-positive cells expressed c-Fos after enteric glucose administration. Importantly, the number of c-Fos/NPY–positive cells, but not POMC cells, was reduced to 10% in response to intragastric glucose. These data point to a potential role of arcuate NPY but not POMC cells in regulating enteric glucose responses. This is consistent with a broad array of evidence that implicates the ARC as an integrator of hormonal and nutrient information to regulate both energy and glucose homeostasis (35,36).

The enteric glucose signal is impaired in high-fat, carbohydrate-free diet–induced diabetes. Diabetic mice are characterized by a state of glucose unresponsiveness. Our data clearly show that mice maintained on a high-fat, carbohydrate-free diet had little change in the number of c-Fos–positive cells in the brain stem in response to intragastric glucose, and this was paralleled by a failure to induce changes in glucose utilization rates. Whether these impairments affect signals arising from the intestine and/or the brain cannot be determined in our study.

In summary, the available data show that the gut-glucose sensor sends signals to the brain that control peripheral glucose utilization in a GLP-1Rc–dependent manner.

REFERENCES

1. Gardemann A, Strulik H, Jungermann K: A portal-arterial glucose concentration gradient as a signal for an insulin-dependent net glucose uptake in perfused rat liver. *FEBS* 202:255–259, 1986
2. Moore MC, Cherrington AD: The nerves, the liver, and the route of feeding: an integrated response to nutrient delivery. *Nutrition* 12:282–284, 1996
3. Hevener AL, Bergman RN, Donovan CM: Novel glucosensor for hypoglycemic detection localized to the portal vein. *Diabetes* 46:1521–1525, 1997
4. Burcelin R, Dolci W, Thorens B: Portal glucose infusion in the mouse induces hypoglycemia: evidence that the hepatoportal glucose sensor stimulates glucose utilization. *Diabetes* 49:1635–1642, 2000
5. Liu M, Seino S, Kirchgessner AL: Identification and characterization of glucoresponsive neurons in the enteric nervous system. *J Neurosci* 19:10305–10317, 1999
6. Adachi A, Shimizu N, Oomura Y, Kobashi M: Convergence of hepatoportal glucose-sensitive afferent signals to glucose-sensitive units within the nucleus of the solitary tract. *Neurosci Lett* 46:215–218, 1984
7. Hollis JH, Lightman SL, Lowry CA: Integration of systemic and visceral sensory information by medullary catecholaminergic systems during peripheral inflammation. *Ann N Y Acad Sci* 1018:71–75, 2004
8. Mithieux G, Misery P, Magnan C, Pillot B, Gautier-Stein A, Bernard C, Rajas F, Zitoun C: Portal sensing of intestinal gluconeogenesis is a mechanistic link in the diminution of food intake induced by diet protein. *Cell Metab* 2:321–329, 2005
9. Holst JJ: The physiology of glucagon-like peptide 1. *Physiol Rev* 87:1409–1439, 2007
10. Nakabayashi H, Nishizawa M, Nakagawa A, Takeda R, Niijima A: Vagal hepatopancreatic reflex effect evoked by intraportal appearance of tGLP-1. *Am J Physiol* 271:E808–E813, 1996
11. Wettergren A, Petersen H, Orskov C, Christiansen J, Sheikh SP, Holst JJ: Glucagon-like peptide-1 7-36 amide and peptide YY from the L-cell of the ileal mucosa are potent inhibitors of vagally induced gastric acid secretion in man. *Scand J Gastroenterol* 29:501–505, 1994
12. Dardevet D, Moore MC, Neal D, DiCostanzo CA, Snead W, Cherrington AD: Insulin-independent effects of GLP-1 on canine liver glucose metabolism: duration of infusion and involvement of hepatoportal region. *Am J Physiol Endocrinol Metab* 287:E75–E81, 2004
13. Ionut V, Hucking K, Liberty IF, Bergman RN: Synergistic effect of portal glucose and glucagon-like peptide-1 to lower systemic glucose and stimulate counter-regulatory hormones. *Diabetologia* 48:967–975, 2005
14. Burcelin R, Da Costa A, Drucker D, Thorens B: Glucose competence of the hepatoportal vein sensor requires the presence of an activated glucagon-like peptide-1 receptor. *Diabetes* 50:1720–1728, 2001
15. Jin SL, Han VK, Simmons JG, Towle AC, Lauder JM, Lund PK: Distribution of glucagonlike peptide I (GLP-I), glucagon, and glicentin in the rat brain: an immunocytochemical study. *J Comp Neurol* 271:519–532, 1988
16. Yamamoto H, Lee CE, Marcus JN, Williams TD, Overton JM, Lopez ME, Hollenberg AN, Baggio L, Saper CB, Drucker DJ, Elmquist JK: Glucagon-like peptide-1 receptor stimulation increases blood pressure and heart rate and activates autonomic regulatory neurons. *J Clin Invest* 110:43–52, 2002
17. Alvarez E, Roncero I, Chowen JA, Thorens B, Blazquez E: Expression of the glucagon-like peptide-1 receptor gene in rat brain. *J Neurochem* 66:920–927, 1996
18. Goke R, Larsen PJ, Mikkelsen JD, Sheikh SP: Distribution of GLP-1 binding sites in the rat brain: evidence that exendin-4 is a ligand of brain GLP-1 binding sites. *Eur J Neurosci* 7:2294–2300, 1995
19. Shimizu I, Hirota M, Ohboshi C, Shima K: Identification and localization of glucagon-like peptide-1 and its receptor in rat brain. *Endocrinology* 121:1076–1082, 1987
20. Larsen PJ, Tang-Christensen M, Holst JJ, Orskov C: Distribution of glucagon-like peptide-1 and other preproglucagon-derived peptides in the rat hypothalamus and brainstem. *Neuroscience* 77:257–270, 1997
21. During M, Cao L, Zuzga D, Francis J, Fitzsimons H, Jiao X, Bland R, Klugmann M, Banks W, Drucker D, Haile C: Glucagon like peptide 1 receptor is involved in learning and neuroprotection. *Nat Med* 9:1173–1179, 2003
22. Goke R, Larsen PJ, Mikkelsen JD, Sheikh SP: Identification of specific binding sites for glucagon-like peptide-1 on the posterior lobe of the rat pituitary. *Neuroendocrinology* 62:130–134, 1995
23. Knauf C, Cani P, Perrin C, Iglesias M, Maury J, Bernard E, Benhamed F, Grémeaux T, Drucker D, Kahn C, Girard J, Tanti J, Delzenne N, Postic C, Burcelin R: Brain glucagon-like peptide-1 increases insulin secretion and muscle insulin resistance to favor hepatic glycogen storage. *J Clin Invest* 115:3554–3563, 2005
24. Perrin C, Knauf C, Burcelin R: Intracerebroventricular infusion of glucose, insulin, and the adenosine monophosphate-activated kinase activator, 5-aminoimidazole-4-carboxamide-1-beta-D-ribofuranoside, controls muscle glycogen synthesis. *Endocrinology* 145:4025–4033, 2004
25. Burcelin R, Crivelli V, Dacosta A, Roy-Tirelli A, Thorens B: Heterogeneous

metabolic adaptation of C57BL/6J mice to high-fat diet. *Am J Physiol Endocrinol Metab* 282:E834–E842, 2002

26. Burcelin R, Crivelli V, Perrin C, Da Costa A, Mu J, Kahn BB, Birnbaum MJ, Kahn CR, Vollenweider P, Thorens B: GLUT4, AMP kinase, but not the insulin receptor, are required for hepatoportal glucose sensor-stimulated muscle glucose utilization. *J Clin Invest* 111:1555–1562, 2003

27. Cani PD, Holst JJ, Drucker DJ, Delzenne NM, Thorens B, Burcelin R, Knauf C: GLUT2 and the incretin receptors are involved in glucose-induced incretin secretion. *Mol Cell Endocrinol* 276:18–23, 2007

28. Burcelin R, Dolci W, Thorens B: Glucose sensing by the hepatoportal sensor is GLUT-2 dependent: in vivo analysis in GLUT-2null mice. *Diabetes* 49:1643–1648, 2000

29. Margolskee RF, Dyer J, Kokrashvili Z, Salmon KS, Ilegems E, Daly K, Maillet EL, Ninomiya Y, Mosinger B, Shirazi-Beechey SP: T1R3 and gustducin in gut sense sugars to regulate expression of Na+-glucose cotransporter 1. *Proc Natl Acad Sci U S A* 104:15075–15080, 2007

30. Preitner F, Ibberson M, Franklin I, Binnert C, Pende M, Gjinovci A, Hansotia T, Drucker DJ, Wollheim C, Burcelin R, Thorens B: Gluco-incretins control insulin secretion at multiple levels as revealed in mice lacking GLP-1 and GIP receptors. *J Clin Invest* 113:635–645, 2004

31. Carlsson PO, Iwase M, Jansson L: Stimulation of intestinal glucoreceptors in rats increases pancreatic islet blood flow through vagal mechanisms. *Am J Physiol* 276:R233–R236, 1999

32. Nishizawa M, Nakabayashi H, Uchida K, Nakagawa A, Niijima A: The hepatic vagal nerve is receptive to incretin hormone glucagon-like peptide-1, but not to glucose-dependent insulinotropic polypeptide, in the portal vein. *J Auton Nerv Syst* 61:149–154, 1996

33. Guillod-Maximin E, Lorsignol A, Alquier T, Pénicaud L: Acute intracarotide glucose injection towards the brain induces specific cFos activation in hypothalamic nuclei: involvment of astrocytes in cerebral glucose sensing in rats. *J Neuroendocrinol* 16:464–471, 2004

34. Yamamoto T, Sawa K: c-Fos-like immunoreactivity in the brainstem following gastric loads of various chemical solutions in rats. *Brain Res* 866:135–143, 2000

35. Kahn BB, Rossetti L: Type 2 diabetes: who is conducting the orchestra? *Nat Genet* 20:223–225, 1998

36. Obici S, Rossetti L: Nutrient sensing and the regulation of insulin action and energy balance. *Endocrinology* 144:5172–5178, 2003

37. Paxinos G, Franklin K: *The Mouse Brain in Stereotaxic Coordinates*. New York, Academic Press, 2001